Journal of Materials and Environmental Sciences
ISSN : 2028-2508
CODEN : JMESCN

J. Mater. Environ. Sci., 2018, Volume 9, Issue 9, Page 2549-2557

http://www.jmaterenvironsci.com

Mineralogical and physicochemical characterization of the Jbel Rhassoul clay deposit (Moulouya Plain, Morocco)

J. Amakrane[1,2*], K. El Hammouti[1], A. Azdimousa[1], M. El Halim[2,3], M. El Ouahabi[2], B. Lamouri[4], N. Fagel[2]

[1]*Laboratoire des géosciences appliquées (LGA), Département de Géologie, Faculté des Sciences, Université Mohammed Premier, BP 717 Oujda, Morocco*

[2]*UR Argile, Géochimie et Environnement sédimentaires (AGEs), Département de Géologie, Quartier Agora, Bâtiment B18, Allée du six Août, 14, Sart-Tilman, Université de Liège, B-4000, Belgium*

[3]*Laboratoire de Géosciences et Environnement (LGSE), Département de Géologie, Faculté des Sciences et Techniques, Université Cadi Ayyad, BP 549 Marrakech, Morocco*

[4]*Laboratoire Géodynamique et Ressources Naturelles(LGRN), Département de Géologie, Faculté des Sciences de la Terre, Université Badji Mokhtar-Annaba, Algeria.*

Received 26 Jan 2018,
Revised 08 Jun 2018,
Accepted 10 Jun 2018

Keywords

- ✓ Clay,
- ✓ Ghassoul,
- ✓ Characterization,
- ✓ Stevensite,
- ✓ Morocco.

jemaa.amakrane@student.uliege.be
Phone: +212641264920
+32465180086

Abstract

This study aims at the mineralogical and physicochemical characterization of clays of the Missour region (Boulemane Province, Morocco). For this, three samples were collected in the Ghassoul deposit. The analyses were carried by X-ray diffraction (XRD), X-ray fluorescence (XRF) and Scanning Electron Microscopy (SEM). The thermal analysis from 500 to1100°C was also performed on studied samples, and the fired samples were characterized by XRD and SEM. The XRD results revealed that raw Ghassoul clay consists mainly of Mg-rich trioctahedral smectite, stevensite-type clay, which represents from 89% to 95% of the clay fraction, with a small amount of illite and kaolinite. The associated minerals are variable amount of quartz, dolomite, hematite, gypsum and K-feldspars. The chemical analysis confirms the presence of Mg-rich smectite (stevensite) with largest amount in sample containing the highest MgO. The SEM micrographs revealed the presence of automorphous structures with petals-like shape typical of smectite. The Thermal transformations determined by X-ray diffraction indicated that stevensite was transformed to enstatite from 800ºC. Diopside starts to appear from 700°C, which is confirmed by SEM observations, and the quartz is transformed to cristobalite when the temperature exceeds 1100°C.

1. Introduction

The Rhassoul deposit from Morocco has a great commercial value in the world. This clay was interpreted as neoformed steveniste (Mg-smectite), in a fresh-water or brackish-water lacustrine environment [1]. It differs from other clays by its very low amount of Al, which allows to be applied to the whole body. North Africa and the Middle East people continued to use it for beauty and as health products. In the middle Age, it was even marriage dowries of girls. Currently, Rhassoul is used around the world (e.g. Tunisia, Europe, USA, Japan and Russia).

Moreover, the Rhassoul, fresh out of the mine is presented as a clay mass of chocolate brown, with conchoidal fracture; it is easily scratched with a knife or simply to the nail. Once dry, it loses the consistency and acquired a shade dull.

The reputation of the "smectite" qualities of Rhassoul is aroused the interest of chemists since the last century. The magnesian smectites are stevensites which have been described previously [2]. Later, the works of Benhammou et al. [3] were showed that the raw Rhassoul clay consists mainly of stevensite, together with the presence of impurities such as quartz and dolomite. Lately, the Rhassoul deposit has been the subject of several tectonic, sedimentological and physico-chemical studies [1, 4-16]. Despite these searches, very limited studies have been carried out for a complete characterization of these materials, particularly their thermal behavior after heating at different temperature.

The aim of this study is to characterize the Rhassoul clay by X-ray diffraction (XRD), X-ray fluorescence spectroscopy (XRF) and scanning electron microscopy (SEM) to evaluate the potential of this local clay deposit, as well as to determine its mineralogical transformation during the firing up to 1100ºC.

2. Materials and Methods

2.1. Materials

2.1.1 Geographical and geological setting

The Rhassoul deposit is located in the Moulouya valley, southwest of the Missour Basin. The later forms a large depression bordered on the south by the High Atlas chains and on the northwest by the Middle Atlas (Figure 1).

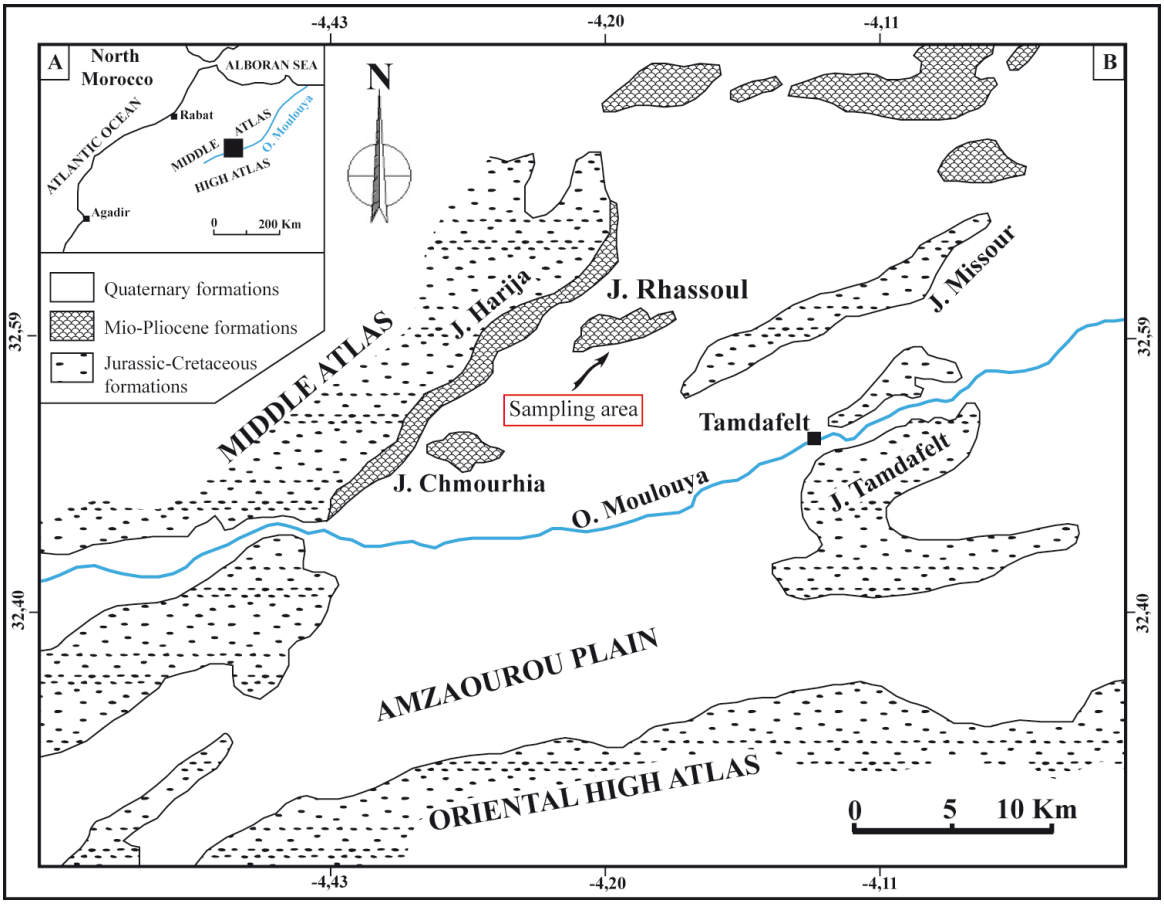

Figure 1: Geographic (A) and geologic (B) setting of the Rhassoul deposit in the Missour Basin [2].

The Missour Basin was formed during the Late Cretaceous and the Cenozoic [17]. The surrection of the Atlas Mountains, have favored the installation of an intra-mountainous basin, which has received a continental sedimentation from the Jurassic-Upper Cretaceous hinterland and Middle Atlas.

In the studied area, the Tertiary deposits of the Missour basin are formed by a large conglomerate series of 200 to 300 m in thick [6, 18]. The deposit is located in the upper part of the Rhassoul series within marly dolomitic facies with a high concentration of gypsum and flint in the center of the basin. According to Benammi and Jaeger [19], the Rhassoul series is of the Miocene age (Figure 1), formed in a lacustrine environment [18]. The series consist of two formations (a) and (b) (Figure 2). The first one (a) is constituted in a dry and confined environment, which confirmed by the presence of gypsum in the fish tail form and the second formation is characterized by marly, clayey and dolomitic levels. A regression affects the basin during the arid period that favored the emergence of the basin and led to the Rhassoul formation at the base (b), and carbonate crusts, with dominance of limestones in strong massif on the surface.

2.2. Methods

The clay samples labeled GH1, GH2 and GH3 were all taken in the intermediate formation of Jbel Rhassoul, this section is characterized by the existence of a small overlay of Rhassoul clays on each other over time. Thus, Figure 3 shows the relative position of samples on the lithological log attributed to [18]. These samples were dried in the oven during 24 hours at 40°C.

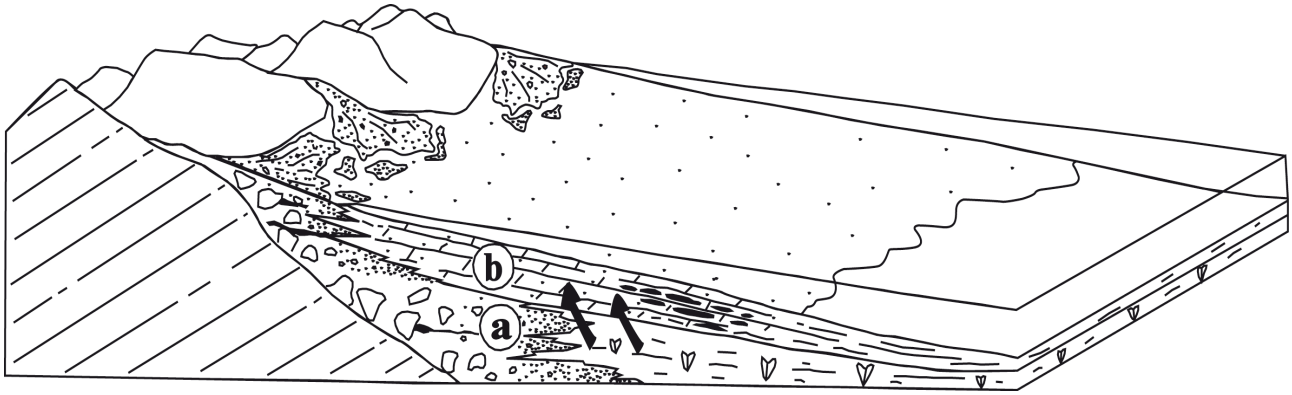

Figure 2: Sedimentary model of the Rhassoul formation and location of the exploited deposit (black levels). Arrows indicate later migration of gypsum from lower (a) to upper formation (b) [1].

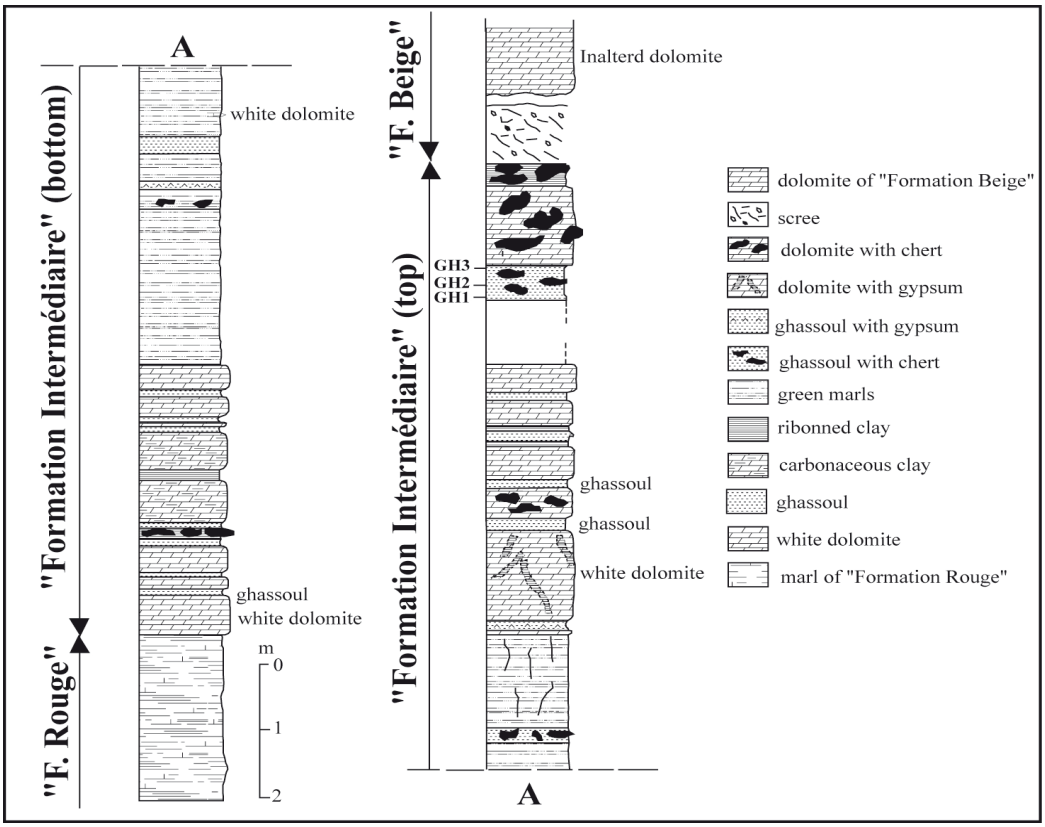

Figure 3: Location of the materials (GH1, GH2, GH3) in the lithological log attributed to Lucas and Prèvôt [18].

The mineralogical composition of the samples was determined [20-21] by X-ray diffraction (XRD) using a Bruker D8-Advance diffractometer with CuKα radiations (AGEs, ULiège). Bulk mineralogy was obtained from powdered samples [22]. For the clay mineralogy, the under 2 μm fraction was separated by settling in a water column. Samples were mounted as oriented aggregates on glass slides [23]. For each sample, three XRD patterns were recorded: air-dried (N), ethylene glycol solvated for 24 h (EG) and heated at 500°C during 4 h (H). The background noise of the XRD patterns was removed and the line position and the peak intensity was calculated using the DIFFRAC plus EVA software (provided by Bruker). Semi-quantitative estimations of the main clay species were obtained on EG runs according to Biscaye [21].

Chemical analysis was determined by X-ray fluorescence spectrometry (XRF) using a Panalytical Axios spectrometer equipped with Rh-tube. Major elements are commonly determined by analysis on glass discs made up by melting and dissolving the sample powder in borate flux [24].

Scanning electron microscopy (SEM) observations on clay samples allow us to examine the microtexture and three-dimensional view of clay minerals. The sample preparation required a thin metallic coating, applied in a vacuum evaporator, which serves to prevent an accumulation of electrons on the sample surface. Within the purpose of following the mineralogical evolution during the firing, the Rhassoul clay samples were dried at 105°C for 24 hours and fired at different temperatures (500°C, 600°C, 700°C, 800°C, 900°C, 1000°C and 1100°C) over 4 hours.

3. Results and discussion

3.1. Mineralogical characterization

The results of the mineralogical analysis (Figures 4 and 5) and (Tables 1 and 2) revealed that the three samples are mostly composed of ~ 77% of the clay fraction, which mainly consists of smectite (89-95%), small amount of illite (3-7%) and traces of kaolinite (< 5%). The associated minerals are k-feldspars (7-15%), quartz (4-7%), and traces of dolomite, enstatite, hematite and gypsum (< 5%).

Table 1: Semi-quantitative estimation, based on X-ray diffraction, of the mineralogical composition of the Rhassoul samples.

Samples	Total clay	K-feldspars	Quartz	Dolomite	Enstatite	Hematite	Gypsum
GH1	+++++	++	+	+	+	+	+
GH2	+++++	++	++	+	+	+	+
GH3	+++++	++	++	++	+	+	+

Key: ++ + + + (75-100%); ++ + + (50-75%); +++ (25-50%); ++ (5-25%); + (<5%)

Table 2: Semi-quantitative estimation of clay (<2µm) mineralogical composition of the Rhassoul samples.

Samples	Smectite	Illite	Kaolinite
GH1	+++++	+	+
GH2	+++++	+	+
GH3	+++++	++	+

Key: ++ + + + (75-100%); ++ + + (50-75%); +++ (25-50%); ++ (5-25%); + (<5%)

The bulk XRD spectra of Rhassoul samples (Figures 4 and 5) represent an intense peak at 14.7Å (5.99º2θ), indicating that the Rhassoul clay is composed mainly of phyllosilicates. The (060) reflection indicates the trioctahedral smectite, showed by a peak at 1.52Å (Figure 6) [3, 8].

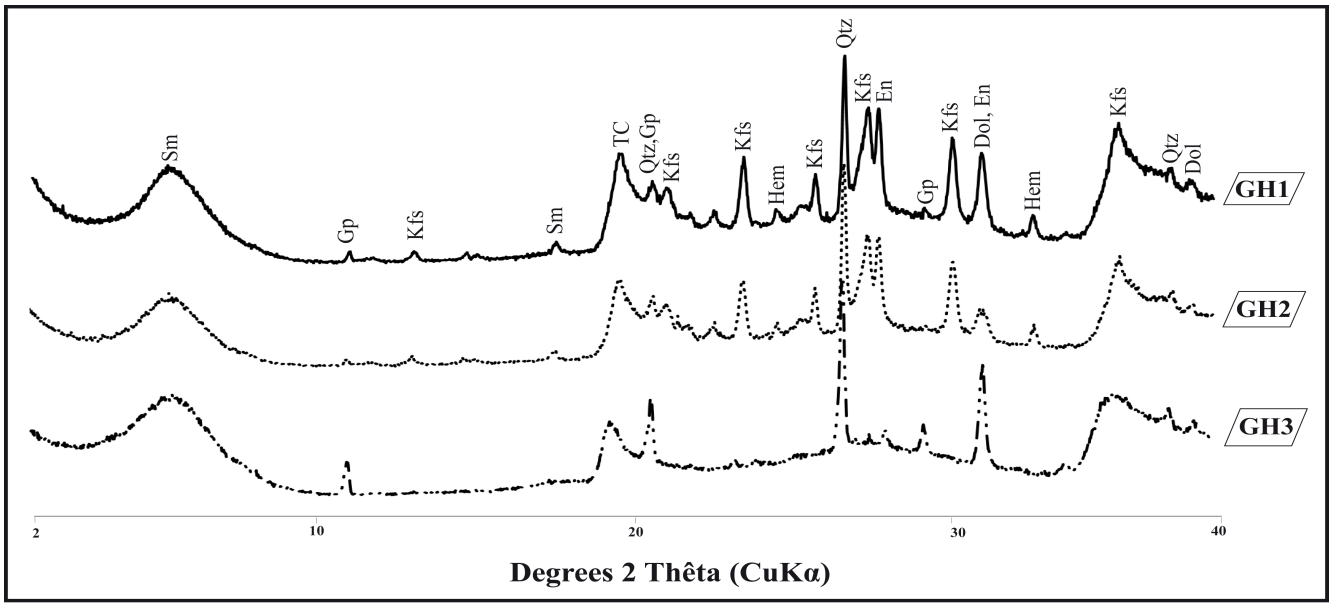

Figure 4: X-Ray diffraction pattern of bulk Rhassoul samples (Qtz: Quartz; Kfs: K-feldspars; Dol: Dolomite; En: Enstatite; Hem: Hematite; Gp: Gypsum; TC: Total clay; Sm: Smectite).

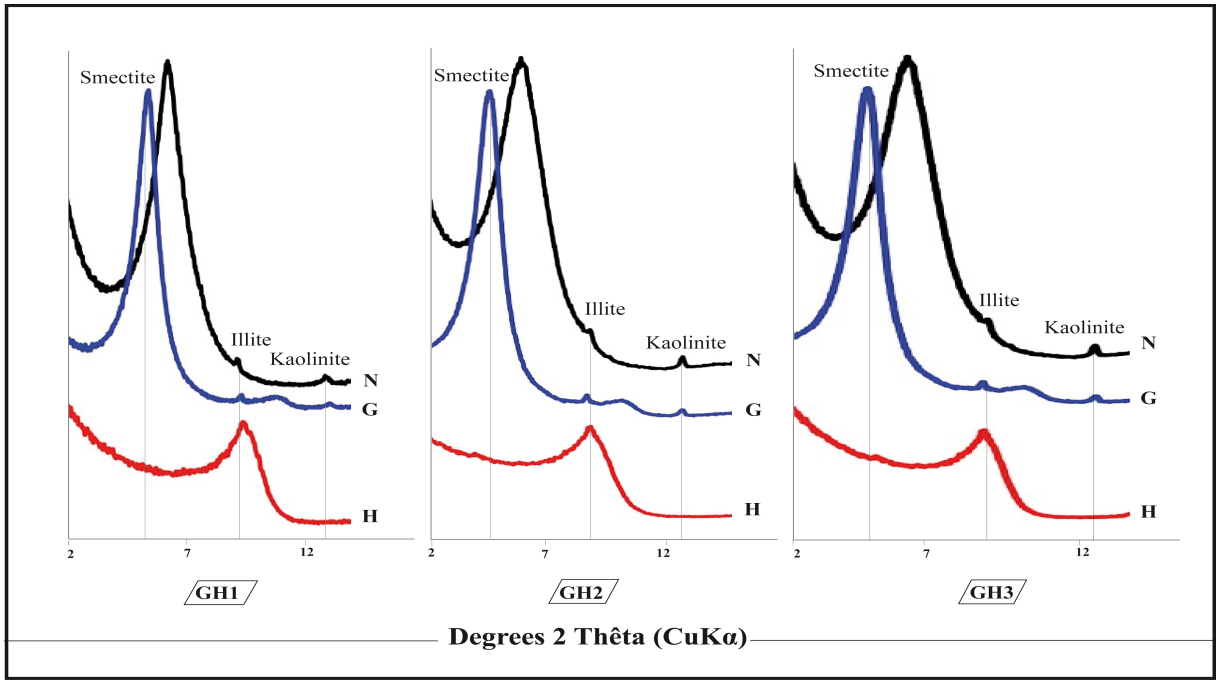

Figure 5: X-ray diffractograms of the studied clay fractions (< 2 µm) with the three different treatments (N: Air dried run; EG: Saturated with ethylene glycol; H: Heated at 500°C for 4h).

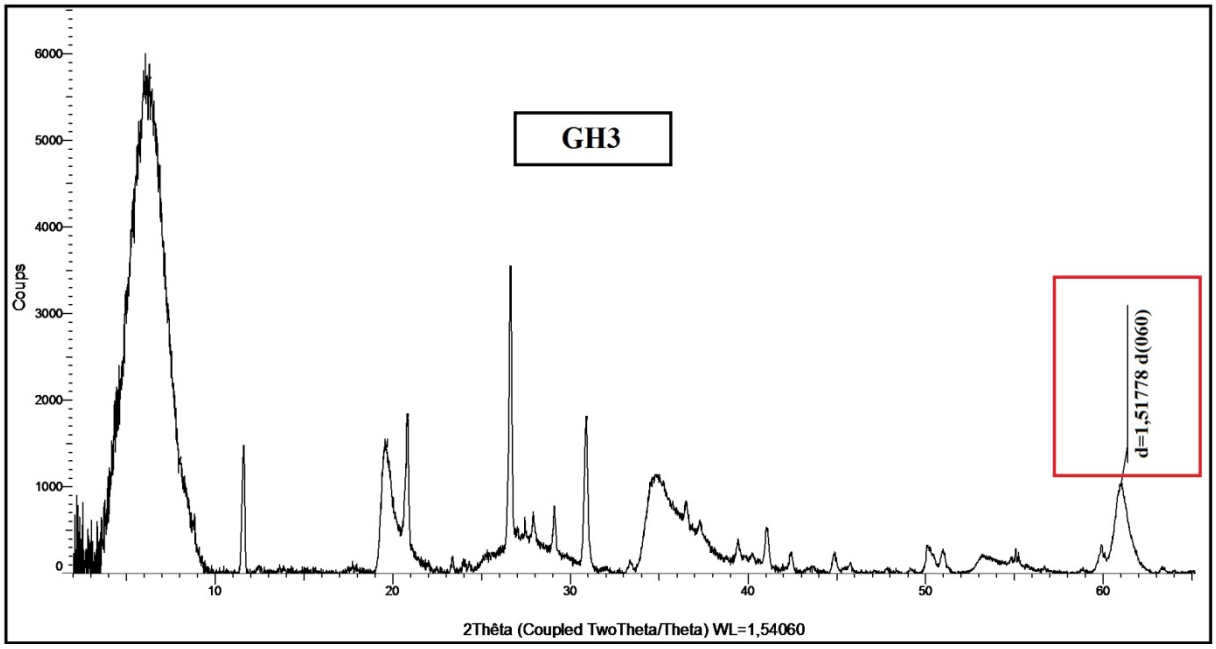

Figure 6: XRD pattern of bulk sample (GH3) showing (060) peak of trioctahedral smectite.

3.2. Physicochemical characterization

3.2.1. Chemical composition

The chemical analyses of the three samples are illustrated in Table 3, the results indicate that the most abundant oxides are silica (SiO_2) associated with magnesium (MgO), alumina (Al_2O_3), iron (Fe_2O_3) and potassium (K_2O), which is in agreement with the mineralogical results. Silica (SiO_2) and alumina (Al_2O_3) reflect the presence of quartz and aluminosilicates (kaolinite and illite). Magnesium (MgO) abundance confirms the presence of Mg-riche smectite as stevensite and dolomite. Iron (Fe_2O_3) is related to the presence of hematite while potassium (K_2O) is binded to the presence of illite and k-feldspars. On the other hand, calcium (CaO) indicates mainly the presence of carbonates (dolomite ~ 6%) and sulfates (gypsum ~ 1.4%), which are reported in the Rhassoul deposit by Chahi et al. [7] and Benhammou [25]. Moreover, GH3 sample is rich in MgO (22.1%) with a low Al_2O_3 content (2.68%), in agreement with the stevensite provided by Faust and Murata [26] and Capet [27].

Table 3: Chemical composition (XRF) of the Rhassoul samples

Sam.	SiO_2	TiO_2	Al_2O_3	Fe_2O_3	MnO	MgO	CaO	Na_2O	K_2O	P_2O_5	L.O.I*	TOTAL
GH1	51.95	0.6	12.26	3.36	0.00	9.83	1.26	0.61	2.2	0.18	16.42	98.67
GH2	53.74	0.82	16.55	4.74	0.00	3.23	0.71	0.96	2.93	0.24	14.57	98.48
GH3	50.81	0.19	2.68	1.14	0.00	22.1	1.66	0.05	0.7	0.05	18.79	98.18

*loss on ignition (1000ºC)…

3.2.2. Microstructural analysis

The SEM observations (Figure 7) confirm the mineralogical results, displaying that smectite is the predominant clay phase in the three samples with an automorphous structure [28].

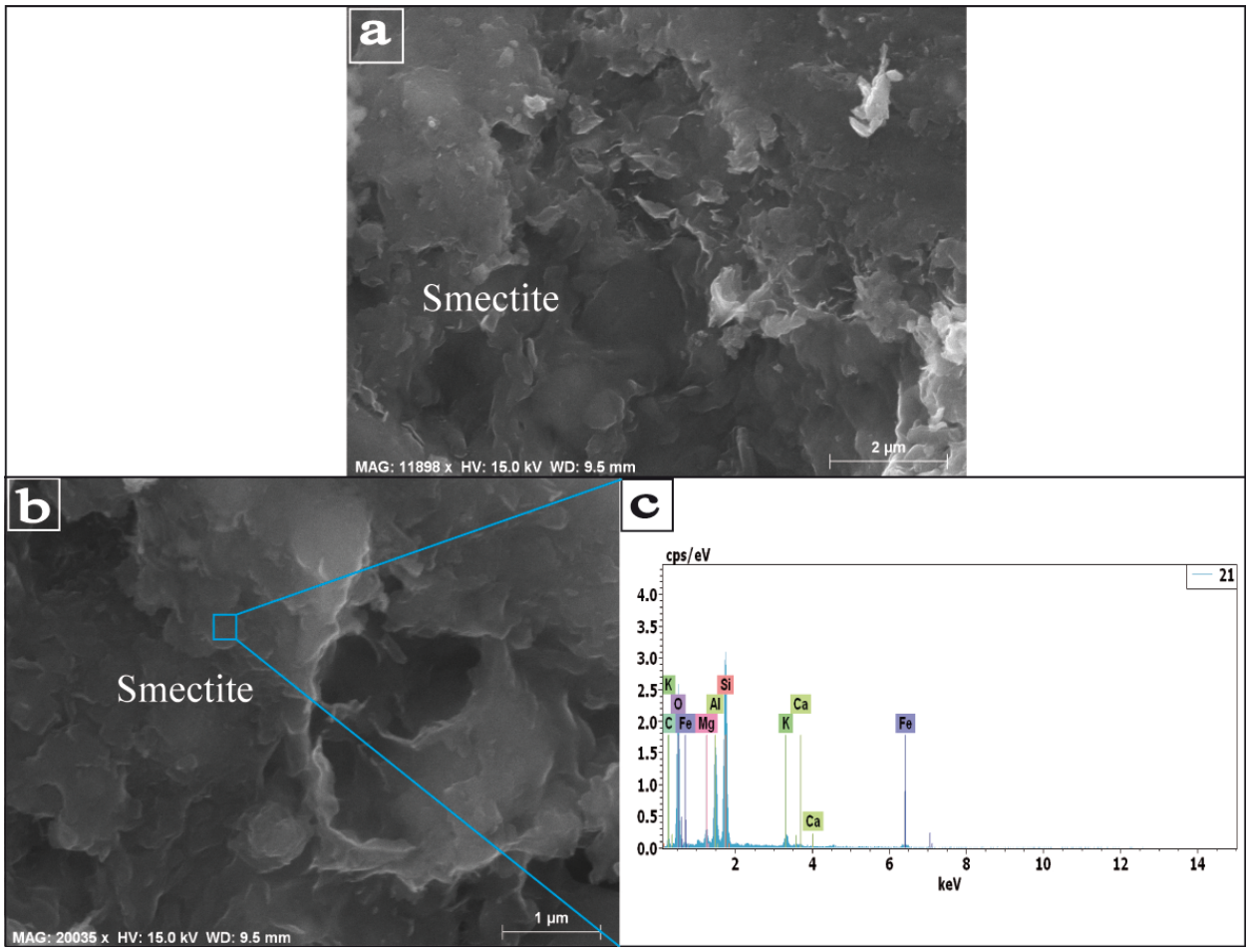

Figure 7: SEM observations of the Rhassoul samples indicate smectite (GH1 and GH2). (a) folded edge petals forming flower structure; (b) Petals gathered in the form of flakes; (c) EDX analysis of the petals.

Petals are present as a flower structure with folded edges (Figure 7a), or taking the form of planar flakes (Figure 7b). EDX analysis of the petals (Figure 7c) is in concordance with the previous chemical analysis. Figure 8 indicates irregular particles of smectite with the presence of indented and flat shape petals; this is related to the slightly saline conditions, marked by the presence of gypsum (~1%) and dolomite (~6%).

3.2.3. Evolution of mineralogical composition during firing

The interactions and physicochemical modifications occurring when clay-rich sediment is fired at high temperatures are a fundamental characteristic of ceramic technology. This process occurs according to several parameters, such as the mineralogical composition of the raw material, its grain-size, firing rate and time, atmosphere of firing [29-32].

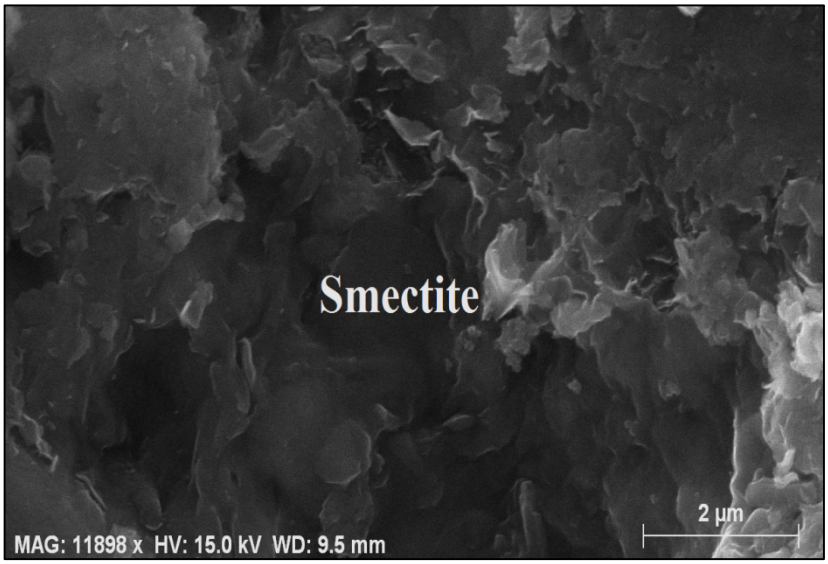

Figure 8: SEM micrograph of the sample (GH3) with indented and flat shape of the smectite petals.

Generally, the first modifications observed during firing are dehydroxylation of kaolinite at 300°C, decomposition of calcite at 700°C and disappearance of other clay minerals (smectite and illite) at temperatures below 950°C [33]. The combination of elements released during firing yields to more stable compounds in the new temperature conditions.

The chemical composition of the argillaceous material is provided on the crystalline phases developed during firing, using the triangular diagrams $SiO_2/Al_2O_3/(NaO_2+K_2O)$ and $SiO_2/Al_2O_3/CaO$ (Figure 9). For the carbonate-rich clays, the first phases formed are gehlenite and diopside between 700°C and 900°C, followed by spinel at 1000°C and wollastonite at 1100°C [34].

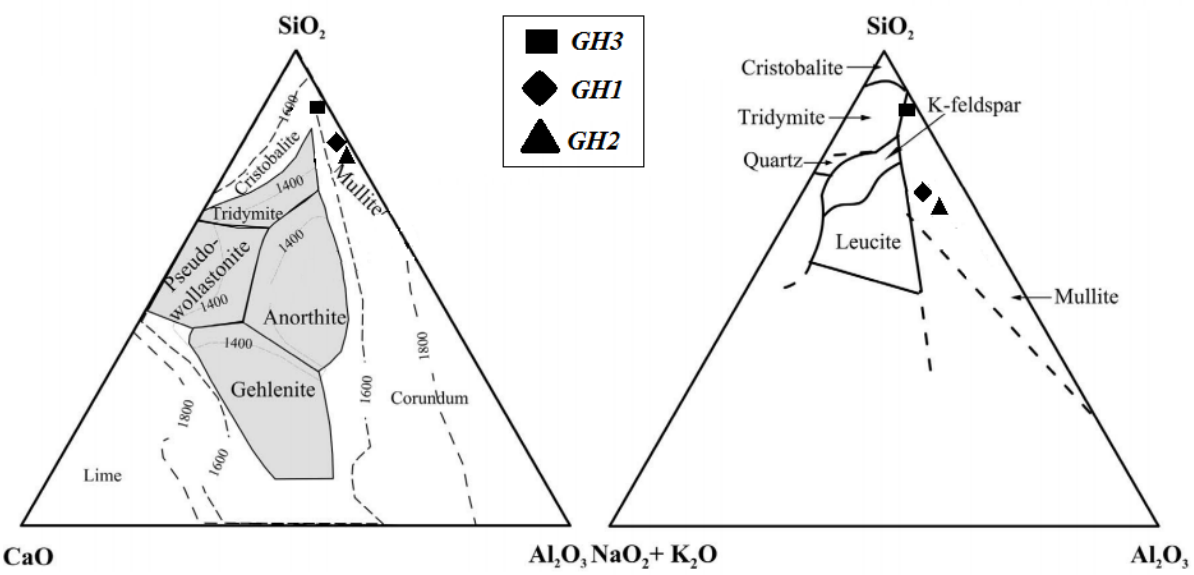

Figure 9: $SiO_2/Al_2O_3/CaO$ and $SiO_2/Al_2O_3/(NaO_2+K_2O)$ equilibrium diagrams [35].

The Rhassoul samples are non-calcareous clays with CaO content not exceed 2%. They appear in the stability domain of mullite and cristobalite on triangular diagrams of Levin (Figure 9). The presence of MgO in these samples (especially in GH1 and GH3) favors the development of the diopside, which begins to appear from 700°C after reaction between dolomite and phyllosilicates rich in magnesium oxide such as stevensite (Figure 11). The peaks of enstatite are twice as great in the samples rich in stevensite at 800°C, on the other hand its content decreases in the sample GH2 and replaced by the appearance of spinel and cristobalite. At 900°C, the spinel derived from the dehydroxylation of smectite [36] develops in the samples (GH1 and GH3) by the reaction (1):

$$MgO + Al_2O_3 \rightarrow MgAl_2O_4 \qquad (1)$$

The spinel content is less developed in the GH3 sample by reason of the low Al_2O_3 content (2%), but the high percentage of MgO favors its formation instead of mullite in all three samples. Quartz is transformed to cristobalite, and marks the start of vitrification from 1100°C (Figure 10). The hematite percentage slightly increased in samples (GH1 and GH2) with moderate contents of Fe_2O_3 (3.4% and 4.7%, respectively).

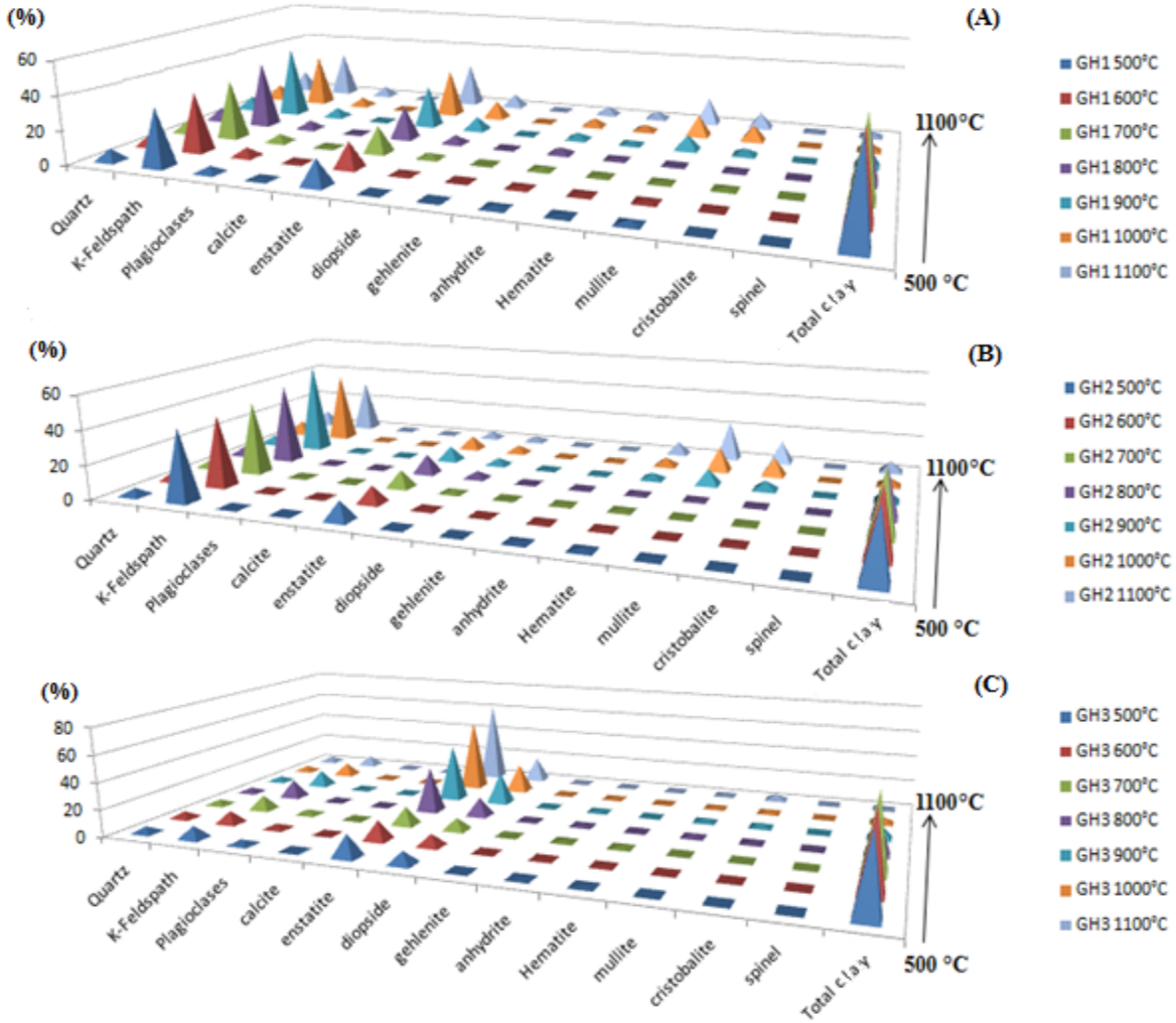

Figure 10: Mineralogical evolution of Rhassoul samples at different firing temperatures (500°C - 1100°C). A : GH1; B : GH2; C : GH3.

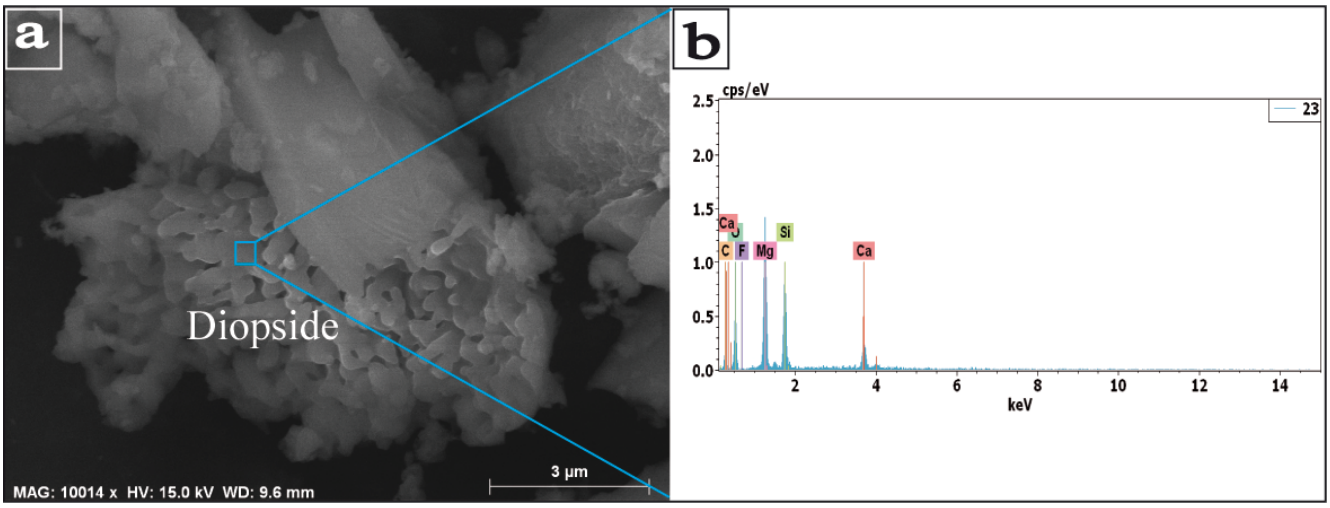

Figure 11: (a) SEM observation of diopside formation in the CaO, MgO and SiO2 interface; (b) EDX analysis of the diopside.

Conclusion

The mineralogical and physicochemical characterization of the clays of Missour region was carried by using various analytical techniques. X-ray diffraction shows that Rhassoul clay is mainly composed of trioctahedral smectite associated with bulk mineralogical assemblages such as quartz, dolomite, gypsum and k-feldspars. This smectite contains the significant amount of Mg (GH3, MgO = 22%) and low content of Al (GH3, Al_2O_3 = 2%), it is phyllosilicates Mg-rich of the stevensite type. Thermal tests have revealed the transformation of stevensite to enstatite and quartz to cristobalite at 800ºC and 1100°C, respectively. XRD and SEM analyses have attested the occurrence of diopside from 700°C.

Acknowledgements - This work was funded by the "Projet de Coopération Bilatérale Wallonie Bruxelles-Maroc (ARES-CCD, Belgium)"; and "Erasmus plus" under Grant Agreement ISCED-F. The authors express their thanks to J. Otten and N. Delmelle for their support for the mineralogical and geochemical analysis.

References

1. P. Duringer, M. Ais, A. Chahi, *Bull. Soc. Géol. Fr.* 166 (1995) 169-179.
2. N. Trauth, *Sci. Géol. Mém*. 49 (1977) 195.
3. A. Benhammou, B. Tanouti, L. Nibou, A. Yaacoubi, J.P. Bonnet, *Clays. Clay. Min.* 57 (2009) 264-270.
4. M. Thiry, M.B. Brahim, *Ecol. Min. Fr.* No: R121208MTHI (2012) 38.
5. E.G. Lafaye, R. Taieb, H. Paquet, A .Chahi, I. Prudencio, *M.A.S. Braga. CR. Acad. Sci. Fr.* 316 (1993) 1239-1245.
6. A. Chahi, *Ph. D. Thesis. Univ. Louis Pasteur.* (1992) 211.
7. A. Chahi, J. Duplay, J. Lucas, *Clays. Clay. Min.* 41 (1993) 401-411.
8. A. Chahi, B. Fritz, J. Duplay, F. Weber, J. Lucas, *Clays. Clay. Min.* 45 (1997) 378-389.
9. A. Chahi, P. Duringer, M. Ais, M. Bouabdelli, F.G. Lafaye, B. Fritz, *J. Sed. Res.* 69 (1999) 1123-1135.
10. B. Rhouta, H. Kaddami, J. Elbarqy, M. Amjoud, L. Daoudi, F. Maury, F. Senocq, A. Maazouz, J.F. Gerard, *Clay. Min.* 43 (2008) 393-403.
11. A. Benhammou, A.Yaacoubi, L. Nibou, B. Tanouti, *Hazar. Mater.* 140 (2007) 104-109.
12. L. Bouna, B. Rhouta, M. Amjoud, A. Jada, F. Maury, L. Daoudi, F. Senocq, *J. optoelect. advan. mater.* 3 (2011) 107-109.
13. O. Qabaqous, N. Tijani, M.N. Bennani, A. El Krouk, *J. Mater. Environ. Sci.* 5 (2014) 2244-2249.
14. Y. Bentahar, C. Hurel, K. Draoui, S. Khairoun, N. Marmier, *App. Clay. Sci.* 119 (2016) 385-392.
15. A. Qlihaa, S. Dhimni, F. Melrhaka, N. Hajjaji, A. Srhiri, *J. Mater. Environ. Sci*. 7 (2016) 1741-1750.
16. K. El Ass, F. Erraib, M. Azzi, A. Laachach, *J. Mater. Environ. Sci.* 9 (2018) 487-496.
17. E. Laville, *Ph. D. Thesis. Univ. Montp.* (1985) 168.
18. J. Lucas, L. Prévôt, *Rap. Int. C.N.R.S.* (1976) 16.
19. M. Benammi, J.J. Jaeger, *Notes. Mém. Soc. Géol. Mar.* 155 (1995) 29-77.
20. H.E. Cook, P.D. Johnson, J.C. Matti, I. Zemmels, *Riverside.* 28 (1975) 999-1007.
21. P.E. Biscaye, *Geol. Soc. Amer. Bull.* 76 (1965) 803-832.
22. G.W. Brindley, G. Brown, *Monog. Min. Soc. Lond.* 5 (1980) 495.
23. D. M. Moore, R.C.J. Reynolds, *Oxford. Univ.* (1989) 1-332.
24. G. Bologne, J.C. Duchesne, *Belg. Geol. Survey. Prof.* 249 (1991) 1-11.
25. A. Benhammou, *Ph. D. Thesis. Univ. Cadi Ayyad.* (2005) 131.
26. G.T. Faust, K.J. Murata, *Amer. Min.* 38 (1953) 973-987.
27. X. Capet, *Ph. D. Thesis. Univ. Sci. Tech. Lille.* (1990) 206.
28. H. Chamley, *Sprin. Verlag. Berlin.* (1989) 623.
29. M. El Ouahabi, L. Daoudi, N. Fagel, *J. Clay. Miner.* 49 (2014) 35-51.
30. G. Cultrone, C.R. Navarro, E.S. Padro, O. Cazalla, M.J. De la Torre, *Eur. J. Min.* 13 (2001) 621-634.
31. J.C. Echallier, S. Mery, *Inst. Géol. (I.G.A.L). Fr.* No: 74 (1989) 55.
32. M. Maggetti, *Archeol. Ceram. (Eds.). J.S. Olin. Smithson. Inst.* (1982) 121-133.
33. G. Cultrone, E. Sebastian, K. Elerta, M.J. De la Torre, O. Cazalla, C.R. Navarro, *J. Eur. Ceram. Soc.* 24 (2004) 547-564.
34. M. Hajjaji, S. Kacim, *Br. Ceram. Trans.* 103 (2004) 29–32.
35. E.M. Levin, C.R. Robbins, H.F. Mc Murdie, *Amer. Ceram. Soc.* 1 (1964) 5-36.
36. M. El Ouahabi, L. Daoudi, F. Hatert, N. Fagel, *Clays. Clay. Min.* 63 (2015) 404–413.